

Supplementary Materials for Identification of genetic outliers due to sub-structure and cryptic relationships

Daniel Schlauch^{1,2}, Heide Fier³, and Christoph Lange^{1,2}

¹Department of Biostatistics, Harvard TH Chan School of Public Health, Boston,
MA 02115

²Department of Biostatistics and Computational Biology, Dana-Farber Cancer
Institute, Boston, MA 02115

³Institute of Genomic Mathematics, University of Bonn, Bonn, Germany

December 30, 2016

1 Supplementary Materials

1.1 Example of $\hat{s}_{i,j}$ computation

Consider a binary matrix of 20 haploid genomes from 10 samples (labeled a-t).

The matrix \mathbf{G} is encoded such that 1 indicates the presence of the minor allele and 0 indicates the presence of the major allele for a particular variant (column) and haploid sample (row). For visual purposes, we limit the calculation to 4 variants and we show \mathbf{G}^T here:

| | a | b | c | d | e | f | g | h | i | j | k | l | m | n | o | p | q | r | s | t |
|-----------|---|---|---|---|---|---|---|---|---|---|---|---|---|---|---|---|---|---|---|---|
| variant 1 | 0 | 0 | 0 | 0 | 0 | 0 | 1 | 0 | 0 | 0 | 0 | 0 | 0 | 1 | 0 | 0 | 0 | 0 | 0 | 0 |
| variant 2 | 1 | 0 | 1 | 0 | 1 | 0 | 1 | 0 | 1 | 0 | 1 | 0 | 1 | 0 | 1 | 0 | 1 | 0 | 1 | 0 |
| variant 3 | 1 | 1 | 1 | 1 | 1 | 1 | 1 | 1 | 1 | 1 | 0 | 0 | 0 | 0 | 0 | 0 | 0 | 0 | 0 | 0 |
| variant 4 | 0 | 0 | 0 | 0 | 0 | 0 | 0 | 0 | 0 | 0 | 1 | 1 | 1 | 1 | 1 | 1 | 1 | 1 | 1 | 1 |

For the purposes of this explanatory example, note that columns g and n share the low frequency allele (1), but differ along the common variants (2-4). Intuitively, we want to consider the relative informativeness of the low frequency variant compared to the common variants.

The minor allele frequencies for variants 1,2,3,4 are 0.1, 0.5, 0.5, and 0.5, respectively.

For each locus, we compute w_k , $k \in \{1, 2, 3, 4\}$

$$w_k = \frac{\binom{20}{2}}{\left(\sum_{l=1}^{20} \mathbf{G}_{l,k}^2\right)}$$

Such that $w_1 = 190$ and $w_2 = w_3 = w_4 = 4.22$

Using equation (1), we compute the relatedness matrix for across these variants:

| | a | b | c | d | e | f | g | h | i | j | k | l | m | n | o | p | q | r | s | t |
|---|-----|-----|-----|-----|-----|-----|------------|-----|-----|-----|-----|-----|-----|------------|-----|-----|-----|-----|-----|-----|
| a | - | 4.2 | 8.4 | 4.2 | 8.4 | 4.2 | 8.4 | 4.2 | 8.4 | 4.2 | 4.2 | 0 | 4.2 | 0 | 4.2 | 0 | 4.2 | 0 | 4.2 | 0 |
| b | 4.2 | - | 4.2 | 4.2 | 4.2 | 4.2 | 4.2 | 4.2 | 4.2 | 4.2 | 0 | 0 | 0 | 0 | 0 | 0 | 0 | 0 | 0 | 0 |
| c | 8.4 | 4.2 | - | 4.2 | 8.4 | 4.2 | 8.4 | 4.2 | 8.4 | 4.2 | 4.2 | 0 | 4.2 | 0 | 4.2 | 0 | 4.2 | 0 | 4.2 | 0 |
| d | 4.2 | 4.2 | 4.2 | - | 4.2 | 4.2 | 4.2 | 4.2 | 4.2 | 4.2 | 0 | 0 | 0 | 0 | 0 | 0 | 0 | 0 | 0 | 0 |
| e | 8.4 | 4.2 | 8.4 | 4.2 | - | 4.2 | 8.4 | 4.2 | 8.4 | 4.2 | 4.2 | 0 | 4.2 | 0 | 4.2 | 0 | 4.2 | 0 | 4.2 | 0 |
| f | 4.2 | 4.2 | 4.2 | 4.2 | 4.2 | - | 4.2 | 4.2 | 4.2 | 4.2 | 0 | 0 | 0 | 0 | 0 | 0 | 0 | 0 | 0 | 0 |
| g | 8.4 | 4.2 | 8.4 | 4.2 | 8.4 | 4.2 | - | 4.2 | 8.4 | 4.2 | 4.2 | 0 | 4.2 | 190 | 4.2 | 0 | 4.2 | 0 | 4.2 | 0 |
| h | 4.2 | 4.2 | 4.2 | 4.2 | 4.2 | 4.2 | - | 4.2 | 4.2 | 4.2 | 0 | 0 | 0 | 0 | 0 | 0 | 0 | 0 | 0 | 0 |
| i | 8.4 | 4.2 | 8.4 | 4.2 | 8.4 | 4.2 | 8.4 | 4.2 | - | 4.2 | 4.2 | 0 | 4.2 | 0 | 4.2 | 0 | 4.2 | 0 | 4.2 | 0 |
| j | 4.2 | 4.2 | 4.2 | 4.2 | 4.2 | 4.2 | 4.2 | 4.2 | 4.2 | - | 0 | 0 | 0 | 0 | 0 | 0 | 0 | 0 | 0 | 0 |
| k | 4.2 | 0 | 4.2 | 0 | 4.2 | 0 | 4.2 | 0 | 4.2 | 0 | - | 4.2 | 8.4 | 4.2 | 8.4 | 4.2 | 8.4 | 4.2 | 8.4 | 4.2 |
| l | 0 | 0 | 0 | 0 | 0 | 0 | 0 | 0 | 0 | 0 | 4.2 | - | 4.2 | 4.2 | 4.2 | 4.2 | 4.2 | 4.2 | 4.2 | 4.2 |
| m | 4.2 | 0 | 4.2 | 0 | 4.2 | 0 | 4.2 | 0 | 4.2 | 0 | 8.4 | 4.2 | - | 4.2 | 8.4 | 4.2 | 8.4 | 4.2 | 8.4 | 4.2 |
| n | 0 | 0 | 0 | 0 | 0 | 0 | 190 | 0 | 0 | 0 | 4.2 | 4.2 | 4.2 | - | 4.2 | 4.2 | 4.2 | 4.2 | 4.2 | 4.2 |
| o | 4.2 | 0 | 4.2 | 0 | 4.2 | 0 | 4.2 | 0 | 4.2 | 0 | 8.4 | 4.2 | 8.4 | 4.2 | - | 4.2 | 8.4 | 4.2 | 8.4 | 4.2 |
| p | 0 | 0 | 0 | 0 | 0 | 0 | 0 | 0 | 0 | 0 | 4.2 | 4.2 | 4.2 | 4.2 | 4.2 | - | 4.2 | 4.2 | 4.2 | 4.2 |
| q | 4.2 | 0 | 4.2 | 0 | 4.2 | 0 | 4.2 | 0 | 4.2 | 0 | 8.4 | 4.2 | 8.4 | 4.2 | 8.4 | 4.2 | - | 4.2 | 8.4 | 4.2 |
| r | 0 | 0 | 0 | 0 | 0 | 0 | 0 | 0 | 0 | 0 | 4.2 | 4.2 | 4.2 | 4.2 | 4.2 | 4.2 | 4.2 | - | 4.2 | 4.2 |
| s | 4.2 | 0 | 4.2 | 0 | 4.2 | 0 | 4.2 | 0 | 4.2 | 0 | 8.4 | 4.2 | 8.4 | 4.2 | 8.4 | 4.2 | 8.4 | 4.2 | - | 4.2 |
| t | 0 | 0 | 0 | 0 | 0 | 0 | 0 | 0 | 0 | 0 | 4.2 | 4.2 | 4.2 | 4.2 | 4.2 | 4.2 | 4.2 | 4.2 | 4.2 | - |

1.2 Expectation of $s_{i,j}$

The expectation of s , under the null of population homogeneity is defined as

$$E[s_{i,j}] = E \left[\frac{\sum_{k=1}^N w_k \mathbf{G}_{i,k} \mathbf{G}_{j,k}}{\sum_{k=1}^N I \left[\sum_{l=1}^{2n} \mathbf{G}_{l,k} > 1 \right]} \right]$$

By this definition and that of w_k , variants which contain one or fewer minor alleles contribute a zero to the summation in both the numerator and denominator and can be ignored. Let N^* be the number of variants indexed k such that $\sum_{l=1}^{2n} \mathbf{G}_{l,k} > 1$, and let k^* index those variants. We condition on the minor allele count for each variant, $a_{k^*} = \sum_{l=1}^{2n} \mathbf{G}_{l,k^*}$, where $n \geq a > 1$,

$$\begin{aligned}
E[s_{i,j}] &= E\left[\frac{\sum_{k^*=1}^{N^*} w_{k^*} \mathbf{G}_{i,k^*} \mathbf{G}_{j,k^*}}{N^*}\right] \\
E[s_{i,j}] N^* &= \sum_{k^*=1}^{N^*} \frac{\binom{2n}{2}}{\binom{a}{2}} E[\mathbf{G}_{i,k^*} \mathbf{G}_{j,k^*}] \\
&= \sum_{k^*=1}^{N^*} \frac{\binom{2n}{2}}{\binom{a}{2}} E[\mathbf{G}_{i,k^*}] E[\mathbf{G}_{j,k^*} | \mathbf{G}_{i,k^*} = 1] \\
&= \sum_{k^*=1}^{N^*} \frac{\binom{2n}{2}}{\binom{a}{2}} \left(\frac{a}{2n}\right) \left(\frac{a-1}{2n-1}\right) \\
&= \sum_{k^*=1}^{N^*} \frac{\frac{2n!}{2!(2n-2)!}}{\frac{a!}{2!(a-2)!}} \left(\frac{a}{2n}\right) \left(\frac{a-1}{2n-1}\right) \\
&= \sum_{k^*=1}^{N^*} \frac{2n(2n-1)}{a(a-1)} \left(\frac{a}{2n}\right) \left(\frac{a-1}{2n-1}\right) \\
&= \sum_{k^*=1}^{N^*} 1 \\
&= N^* \\
E[s_{i,j}] &= 1
\end{aligned}$$

Intuitively, we can consider the weight factor, w_k , to be the inverse of the probability of selecting two minor alleles at random without replacement. Therefore, the expectation for the numerator for each variant is one, and consequently, $s_{i,j}$, the mean over all variants with multiple minor alleles is also one.

1.3 Variance of $s_{i,j}$

The variance of $s_{i,j}$ can be estimated by

$$\sigma_{i,j}^2 = \hat{Var}(s_{i,j}) = \frac{\sum_{k=1}^N (w_k - 1)}{\left(\sum_{k=1}^N I\left[\sum_{l=1}^{2n} \mathbf{G}_{l,k} > 1\right]\right)^2}$$

This formulation is independent of the samples i, j and depends only on the allele counts for each variant across the study group.

$$\begin{aligned}
Var(s_{i,j}) &= Var\left(\frac{\sum_{k=1}^N w_k \mathbf{G}_{i,k} \mathbf{G}_{j,k}}{\sum_{k=1}^N I\left[\sum_{l=1}^{2n} \mathbf{G}_{l,k} > 1\right]}\right) \\
&= \left(\sum_{k=1}^N I\left[\sum_{l=1}^{2n} \mathbf{G}_{l,k} > 1\right]\right)^{-2} Var\left(\sum_{k=1}^N w_k \mathbf{G}_{i,k} \mathbf{G}_{j,k}\right) \\
&= \left(\sum_{k=1}^N I\left[\sum_{l=1}^{2n} \mathbf{G}_{l,k} > 1\right]\right)^{-2} \sum_{k=1}^N Var(w_k \mathbf{G}_{i,k} \mathbf{G}_{j,k}) && \text{Independence of variants} \\
&= \left(\sum_{k=1}^N I\left[\sum_{l=1}^{2n} \mathbf{G}_{l,k} > 1\right]\right)^{-2} \sum_{k=1}^N w_k^2 Var(\mathbf{G}_{i,k} \mathbf{G}_{j,k}) \\
&= \left(\sum_{k=1}^N I\left[\sum_{l=1}^{2n} \mathbf{G}_{l,k} > 1\right]\right)^{-2} \sum_{k=1}^N w_k^2 P[\mathbf{G}_{i,k} \mathbf{G}_{j,k} = 1] (1 - P[\mathbf{G}_{i,k} \mathbf{G}_{j,k} = 1]) && \text{Variance of Bernouli RV} \\
&= \left(\sum_{k=1}^N I\left[\sum_{l=1}^{2n} \mathbf{G}_{l,k} > 1\right]\right)^{-2} \sum_{k=1}^N w_k^2 \frac{1}{w_k} \left(1 - \frac{1}{w_k}\right) \\
&= \frac{\sum_{k=1}^N (w_k - 1)}{\left(\sum_{k=1}^N I\left[\sum_{l=1}^{2n} \mathbf{G}_{l,k} > 1\right]\right)^2}
\end{aligned}$$

1.4 Linkage Disequilibrium Pruning

Phase 3 of the 1000 Genomes Project contains 2504 individuals with a combined total of over 80 million variants. Assumptions of STEGO include the independence of variants, which may be violated in the presence of Linkage Disequilibrium (LD). Our method focuses variants with low minor allele frequency, which are less susceptible to high R^2 between loci. However, to help reduce the impact of correlated variants, we filtered the data such that the impact of LD was limited. Prior to analysis, we divided the data into blocks of 800 consecutive variants and selected only one locus from each block. The selected variant within each block was chosen based on the smallest minor allele frequency observed which was larger than our cutoff of 1% (see Supplemental Materials 1.5). We chose this somewhat arbitrary cutoff as a compromise between our desire to focus on rare alleles and the recognition that QC concerns may become an increasingly valid concern at the lowest allele frequencies. We recommend the use of a cutoff which balances the value of rare variants with the confidence in the technology used to obtain the data. This filtering yielded approximately 100,000 variants for each of the 26 populations in the TGP.

1.5 STEGO algorithm computation time

Of interest is the computation time of STEGO in comparison to other similarity metrics. Principal Components Analysis can be performed in multiple ways, including a decomposition of the correlation or covariance matrix and a singular value decomposition, implemented in base R as the functions `prcomp()` and `princomp()`, respectively. We compared our method in terms of

computation time of generating a correlation matrix. We simulated a study of $p = 100,000$ phased variants across N individuals and ran an R implementation of STEGO against the base implementation of correlation, `cor()` and the two Principal Components analysis methods with default parameters (Supplemental Figure 6). An R script implementing this simulation is available at <https://github.com/dschlauch/Genetic-Outliers/blob/master/timingComparison.R>. Using a computer with Intel(R) Core(TM) i7-3630QM CPU @ 2.40GHz, and Microsoft R Open 3.2.5 linked with multi-threaded BLAS/LAPACK libraries, we found that our method ran substantially faster than correlation (`cor`) and PCA (`princomp`) in R.

STEGO’s weights are independently computed for each of the p variants based solely on the minor allele count and thus are computed in linear time, $\mathcal{O}(p)$. The computationally intensive step is implemented via matrix multiplication of the weighted genotypes matrix, which with naive implementation has complexity $\mathcal{O}(pN^2)$. Both singular value decomposition and variance-covariance matrix computations have complexity $\mathcal{O}(pN^2)$ [1], and therefore each of the three methods compared have the same asymptotic computational complexity.

1.6 Ancestry informativeness by allele frequency

An important motivating principle of our method is the assertion that rare variants are useful for identifying fine-scale population structure. The reasoning is that rare variants are less stable than common variants and can more easily become fixed at 0%. It is reasonable to suspect that rare variants are more likely to have arisen recently in the ancestral history of a population and may therefore be informative in separating recently related populations.

To confirm this concept in the 1000 Genomes Project, we compared the relative abilities of MAF bins to separate populations. We used the Jaccard Index to compute a similarity score between all pairs of individuals and computed the ratio of within-population to between-population Jaccard Index means. Figure 2 shows the comparison of the Yoruban population (YRI) with all others and demonstrates the improved performance of rare variants compared with more common variants. It is notable, however, that the improvement clearly ceases at the lowest MAF bin (0%-0.4%), suggesting a lack of reliability for the rarest variants as a result of the imperfect nature of sequencing. It is for this reason that we recommend a minimum MAF for analyses which considers features of the analysis such as sequencing depth.

1.7 Simulations demonstrate sensitivity STEGO to subtle population stratification

We compared the GSM derived from STEGO against a GSM obtained via normalized variance-covariance, such as that used in EIGENSTRAT’s implementation of PCA [2]. We first generated an ancestral allele frequency distribution for 20k variants, each as an observation from an *exponential* ($\lambda = .05$) distribution. Next, two descendant allele frequencies were obtained by applying a small deviation from the ancestral allele frequency of *Uniform* ($-0.003, 0.003$). The purpose was to create a very subtle genetic drift loosely representing a relatively short timeframe of breeding isolation for each population. We chose the size of small allele frequency deviation as one which pushes the limits of standard approaches to detect. The 1000 simulated individuals were sampled independently from the descendant allele frequencies (500 from each population), and GSMs were generated as described above.

The results from this straightforward simulation support our intuition regarding rare variants (Supplemental Figure 7). Owing to the fact that co-occurrence of rare variants is more informative of shared population membership than co-occurrence of common variants, we see that STEGO outperforms standard PCA in this scenario. In this plot, using the top two eigenvectors shown, the ratio of within-population variance to total variance is .81 for STEGO. For variance-covariance, this ratio is .99, as this standard method was ineffective at picking up virtually any signal. At this level of subtle population stratification and using only 20k variants, we do not observe any meaningful separation between the two groups using PCA. Conversely, STEGO clearly demonstrates a tendency to distinguish the groups along the first principal component. The source code for this simulation is available at https://github.com/dschlauch/Genetic-Outliers/blob/master/simulated_stego_varcov.R.

1.8 Simulations demonstrate power to detect heterogeneity

We ran STEGO on simulated genotypes derived from a homogeneous dataset containing varying degrees of relatedness. A homogenized version of a real dataset was generated by randomly re-sampling each variant across all samples. This eliminates correlations between individuals and variants, preserving only the allele frequency distribution. To test the power of our method to identify relatedness we generated an additional sample, S_{N+1} which was related to an arbitrarily chosen individual, S_N , in the homogenized dataset. The genotype for S_{N+1} was generated by assigning one of their values for each allele to be the same as one of the alleles of S_N with probability 4ϕ and assigning the other to be a randomly chosen allele across all samples. With probability $1 - 4\phi$, both haplotypes for S_{N+1} were selected randomly from the homogenized data.

For variant i , allele j , the genotype at $S_{N+1,i,j}$ is given as

$$S_{N+1,i,j} = \begin{cases} S_{N,i,1} & \text{with probability } \phi + \frac{1-2\phi}{2N} \\ S_{N,i,2} & \text{with probability } \phi + \frac{1-2\phi}{2N} \\ S_{1,i,1} & \text{with probability } \frac{1-2\phi}{2N} \\ \vdots & \vdots \\ S_{N-1,i,2} & \text{with probability } \frac{1-2\phi}{2N} \end{cases}$$

For each coefficient of kinship we simulated 1,000 studies containing 301 individuals across 100,000 variants in the above manner to evaluate the power of STEGO. Each simulated study contained only a single related pair with relatedness, ϕ , among an otherwise homogeneous dataset. We demonstrate that under the null hypothesis, $H_0 : \phi = 0$, the family-wise type I error rate, $\alpha = .05$ is preserved. We then compared the proportion of simulated studies which were found to have significantly related pairs to the analytically derived probability of type II error. Figure ?? demonstrates that our findings that computed Type II error aligns to the formula in Equation 7. Further investigation into the computational complexity of our method show that our method does not sacrifice speed compared to standard PCA (see Supplemental Materials 1.7).

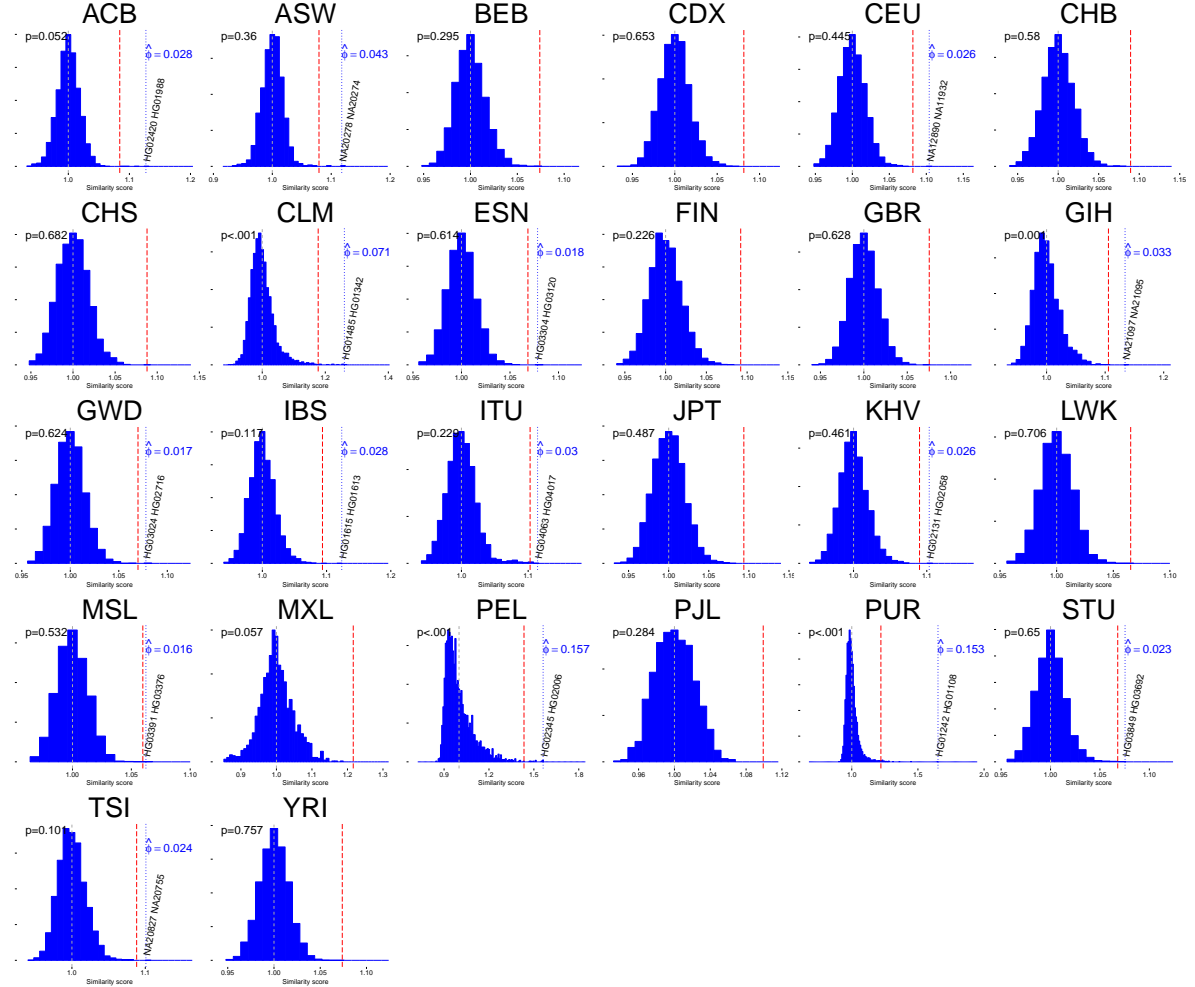
References

- [1] Michael Holmes, Alexander Gray, and Charles Isbell. Fast svd for large-scale matrices. In Workshop on Efficient Machine Learning at NIPS, volume 58, pages 249–252, 2007.

- [2] Alkes L Price, Nick J Patterson, Robert M Plenge, Michael E Weinblatt, Nancy A Shadick, and David Reich. Principal components analysis corrects for stratification in genome-wide association studies. Nature genetics, 38(8):904–909, 2006.

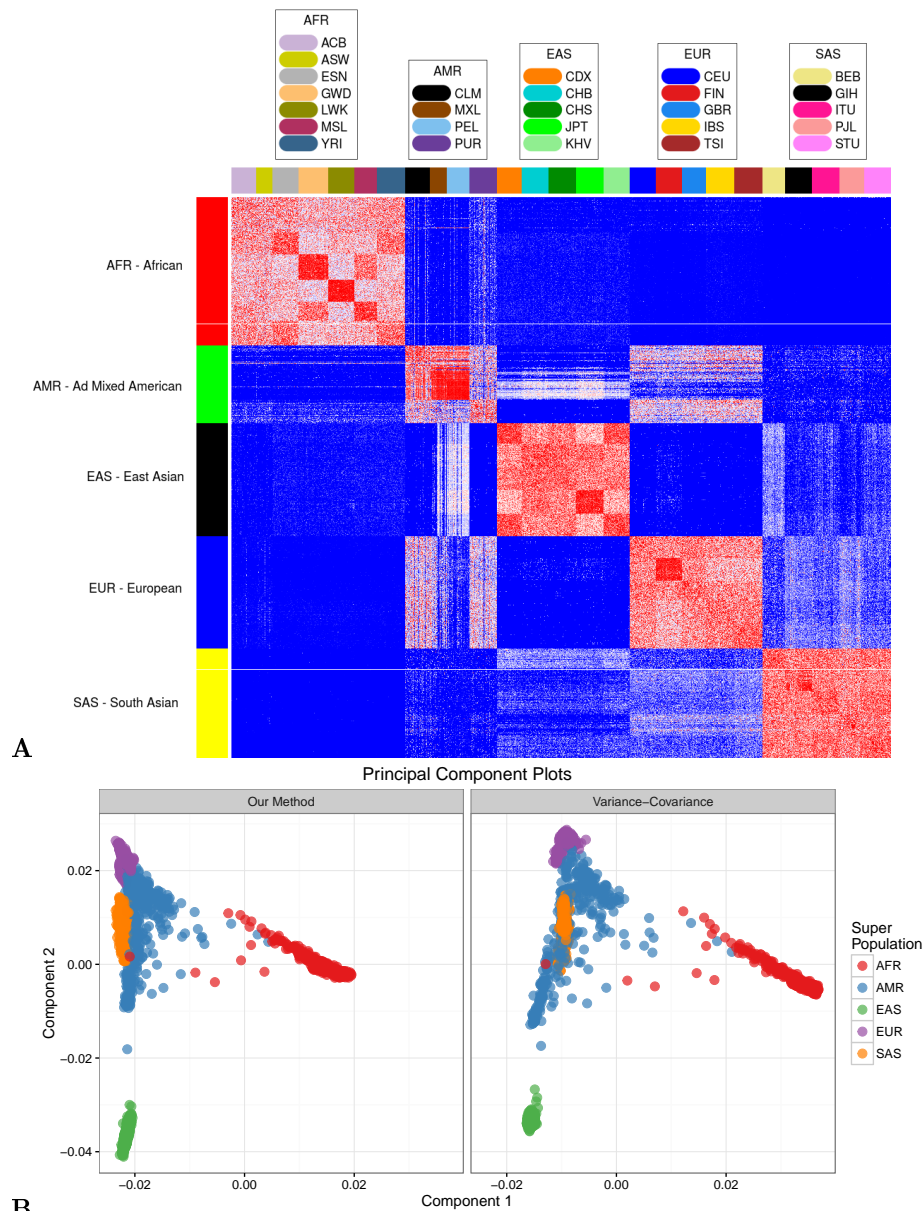
2 Supplementary Figures

Distribution of similarity statistic within population subgroups from 1000 Genomes Project after removal of related individuals

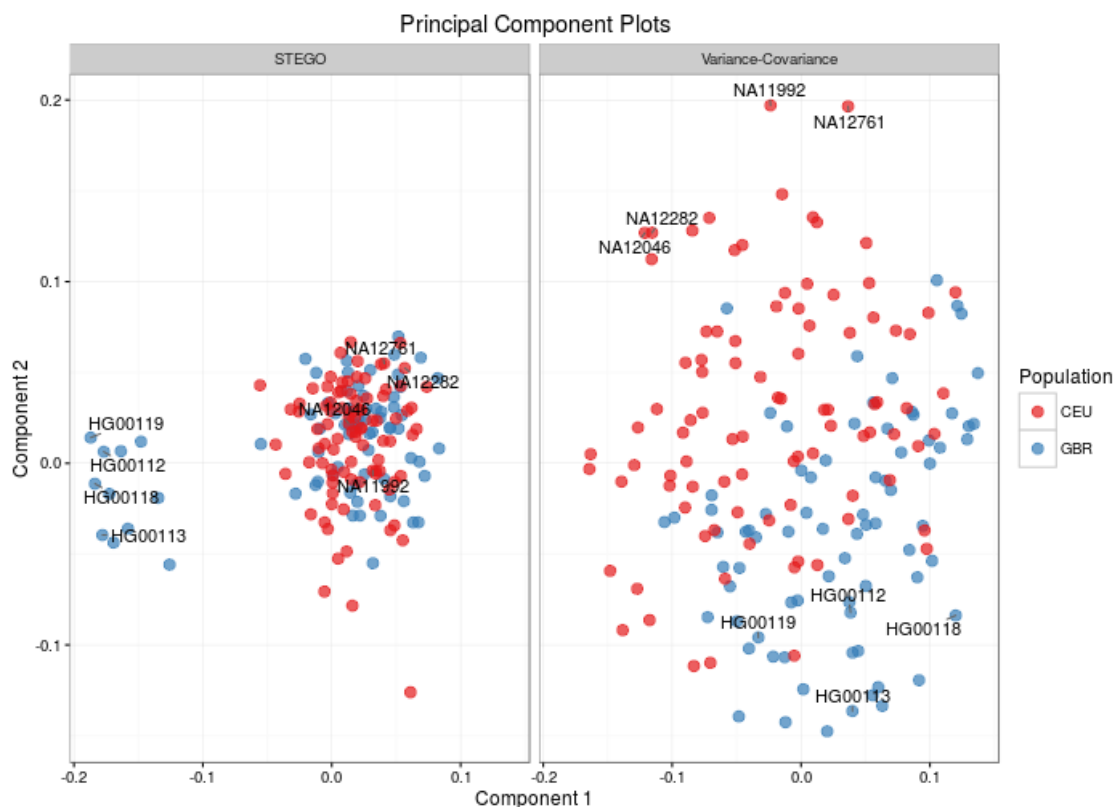


Supplemental Figure 1: Distribution of similarity coefficients for each of the 26 populations in the 1000 Genomes Project after the removal of suspected related individuals. Homogeneous populations lacking cryptic relatedness should be expected to exhibit distributions centered around 1 with no outliers. A heterogeneous population is expected to exhibit a normal distribution centered around 1. Non-normal distributions such as right-skewed (e.g. PUR, PEL, CLM) or bimodal are indicative of population structure. The red dotted vertical line on each plot indicates the family-wise $\alpha = .01$ level cutoff for $\binom{n}{2}$ comparisons. The most significant related pair is labeled for each population with the estimated kinship for that pairing indicated in blue. The p-value for the KS test for homogeneity is reported for each population. Outliers in the absence of non-normally distributed statistics are an indication of relatedness among pairs of individuals.

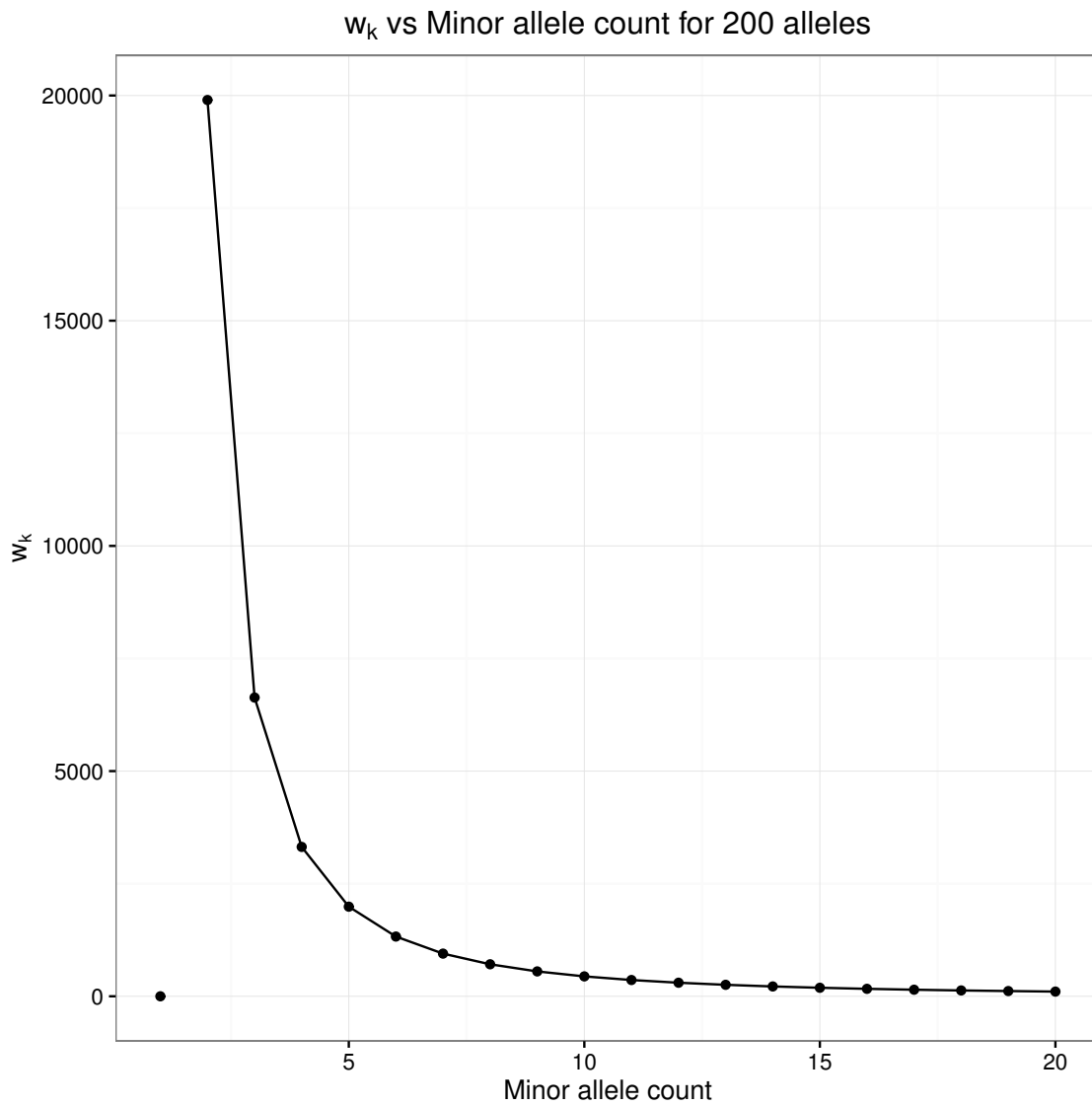
Genetic Similarity Matrix



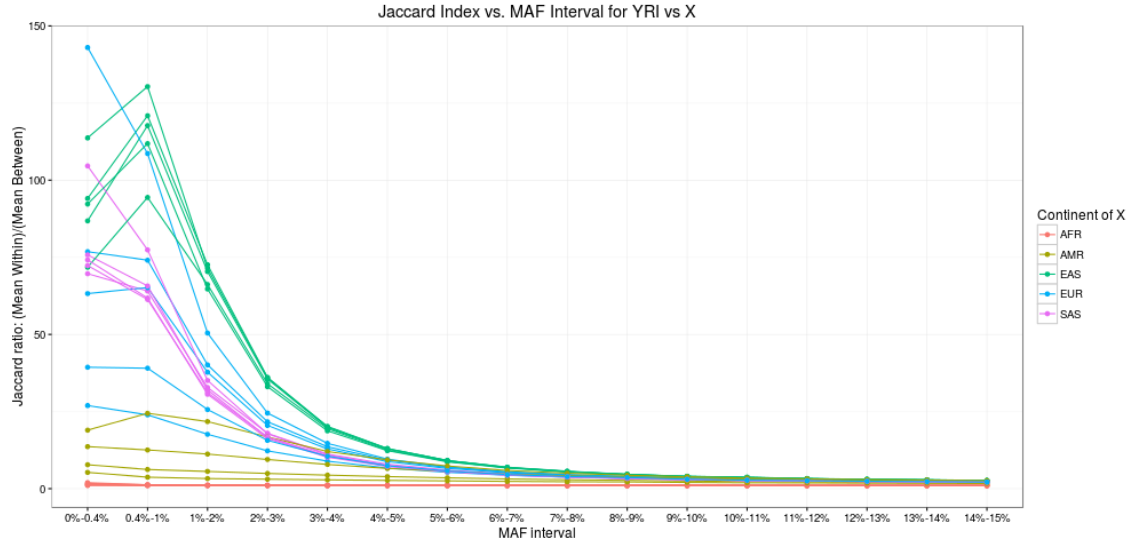
Supplemental Figure 2: Population structure in 2504 samples from 1000 Genomes Project. **(A)** Heatmap of the GSM generated by STEGO using 80,000 LD-sampled variants. The vertical colorbar indicates membership in one of the five superpopulations, while the horizontal colorbar indicates membership in one of the 26 populations. **(B)** Projecting each individual onto the top two eigenvectors resulted in a similar 2-dimensional distribution of global ancestry. Both STEGO and PCA show similar projections which elucidate the migratory patterns of early humans.



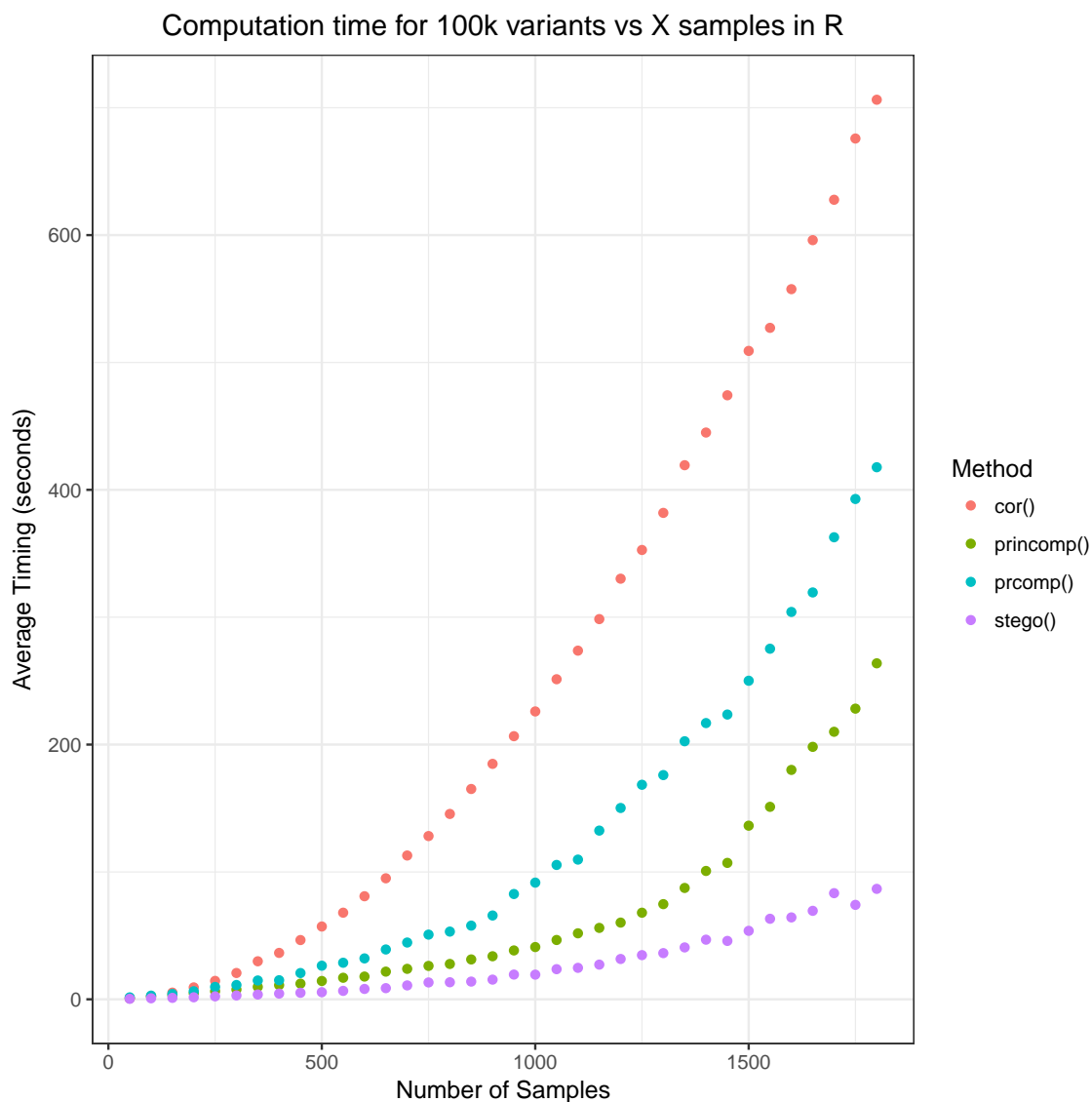
Supplemental Figure 3: Despite a clear trend of superior performance with STEGO, notable exceptions occur. For example, by this measure, the populations GBR and CEU were more clearly divided by PCA (Right) than by STEGO (Left). Closer inspection revealed that the first eigenvector from STEGO isolates 11 samples exclusively from the GBR population. It is not readily apparent what features of the data are being captured here or the relative value of those features (this may be a result of population structure, relatedness, batch effect, etc.). But it is notable that all 11 samples came from the same population in the 1000 Genomes Project. It is reasonable to infer that this subset of samples is scientifically relevant. It most likely contains a disproportionate number of co-occurrences of rare variants, which were not observed separately by PCA.



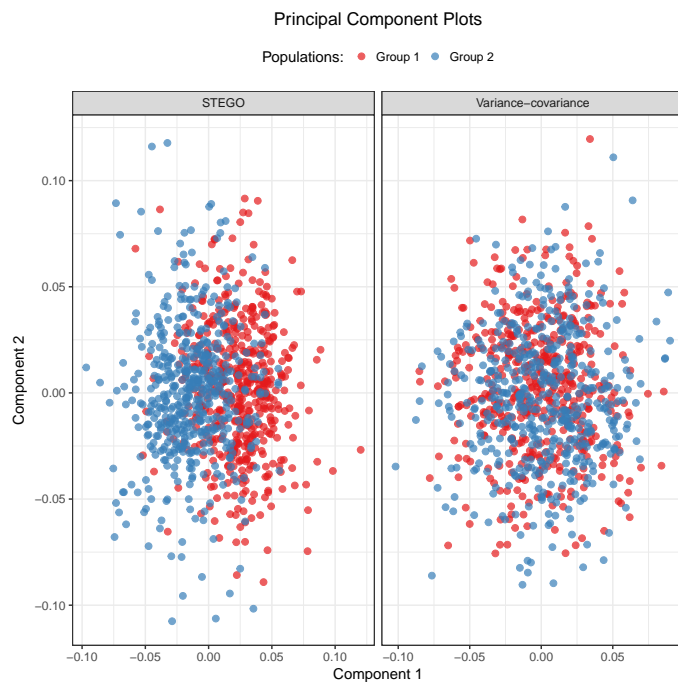
Supplemental Figure 4: The weight factor, w_k , is shown here as a function of the minor allele count in an example of 100 individuals (200 alleles) for each locus, k . w_k is monotonically decreasing for minor allele counts greater than 1, lending greater power to lower frequency variants. Typically, there will be a minimum minor allele count such that the largest values for w_k are never obtained in practice



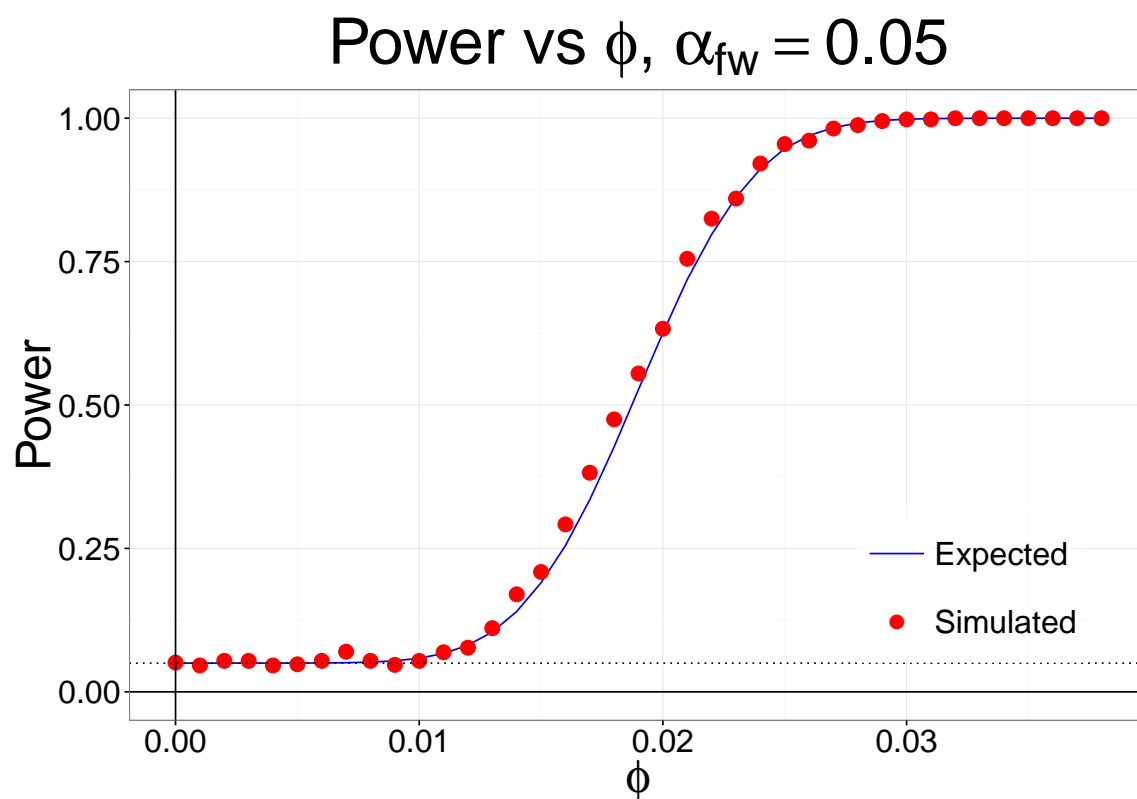
Supplemental Figure 5: **Lower frequency alleles are more informative of ancestry.** For the Yoruban population (YRI), this plot compares the average unweighted Jaccard Index between individuals within group to individuals in all other populations of the 1000 Genomes Project. When filtering by each minor allele frequency, we observe that low frequency alleles create the strongest separation between populations. This trend holds true for all but the lowest interval (0-0.4% MAF), likely owing to a tradeoff between rare variant informativeness and quality control reliability.



Supplemental Figure 6: **Average running time of STEGO is compared to the default implementations of cor() and princomp() in R.** For each sample size on the x-axis, 100,000 variants were randomly generated across the samples. R functions for STEGO, correlation, and two implementations of PCA (**prcomp** and **princomp**) were run 10 times on each simulated dataset. Each of these methods has asymptotic computational complexity of $\mathcal{O}(pN^2)$, and we observe a consistent speed improvement of approximately 3x for STEGO compared to **princomp()**. This improvement scales linearly with increased number of variants, which is most appealing for large whole genome sequencing studies involving thousands of subjects and millions of variants.



Supplemental Figure 7: Principal Component plots for two methods for generating the genetic similarity matrix. On the left, the GSM is generated via STEGO and on the right the GSM uses the normalized covariance matrix. The STEGO method makes more efficient use of the more ancestry informative rare variants, providing a higher resolution separation of our two closely related populations. Across the first two components the ratio of within-population variance to total variance for STEGO vs variance-covariance is .81 and .99, respectively.



Supplemental Figure 8: The probability of rejecting the null hypothesis given a simulated set of 301 homogeneous individuals containing a single related pair with coefficient of kinship, ϕ . The simulated power curve aligns with the analytically derived expectation demonstrating the clearly defined power of the method.